TRENDS IN SCIENCES 2026; 23(9): 13021
https://doi.org/10.48048/tis.2026.13021 RESEARCH ARTICLE

Marine Collagen–Chitosan Composite from Fishery By-Products for Wound Dressing: Characterization and Antibacterial Activity

Sitti Hardiyanti Rachman[1,*], Mila Safitri Rizfa[2], Shanca Kusumo[1], Syarifah Nafhastus Sehroh[1], Iskarimah Atqiah[1], Rachmat Hidayat[3] and Fahri Sinulingga[4]

[1]Department of Fisheries Product Technology, Faculty of Fisheries and Marine Science, Lambung Mangkurat University,South Kalimantan 70714, Indonesia
[2]Department of Marine Science, Faculty of Fisheries and Marine Science, Lambung Mangkurat University, South Kalimantan 70714, Indonesia
[3]Departemen of Fisheries, Faculty of Marine Science and Fisheries, Hasanuddin University, South Sulawesi 90245, Indonesia
[4]Study Program of Fisheries Product Technology, Faculty of Agricultural, Sriwijaya University, South Sumatra 30662, Indonesia

([*]Corresponding author's e-mail: sthardiyantirachman@ulm.ac.id)

Received: 14 December 2025, Revised: 10 February 2026, Accepted: 17 February 2026, Published: 1 April 2026

Abstract

Fishery by-products represent a sustainable source of marine biomaterials with significant potential for wound dressing applications. This study investigates a marine collagen–chitosan composite derived from Spanish mackerel skin and blue swimming crab shells as a candidate wound dressing material, with a focus on structural characterization and antibacterial activity. Acid-soluble collagen (ASC) was extracted through alkaline pretreatment followed by acetic acid hydrolysis, yielding 3.125%, and the freeze-dried product exhibited a porous white morphology with well-preserved amide bands. SEM–EDX analysis revealed a distinct transformation from the dense dermal matrix of raw skin to a layered ASC structure dominated by carbon and oxygen elements, indicating improved collagen purity. Chitosan obtained from blue swimming crab shells achieved a 19.3% yield, moderate viscosity (65.3 mPa·s), and a high degree of deacetylation (92.57%). FTIR and EDX characterization confirmed the successful removal of acetyl groups and a substantial reduction in mineral elements. Antibacterial assays demonstrated that pure chitosan exhibited inhibitory activity against *Escherichia coli* (18.23 ± 0.20 mm) and *Staphylococcus aureus* (15.80 ± 1.65 mm), while collagen–chitosan composites retained activity against *E. coli* but showed reduced effectiveness against *S. aureus*. These results demonstrate the feasibility of utilizing locally derived marine collagen and chitosan as a composite biomaterial, with antibacterial performance influenced by chitosan proportion and requiring further formulation optimization.

Keywords: Fishery by-product utilization, Marine collagen–chitosan composite, Acid-soluble collagen, Antibacterial biomaterials, Wound dressing materials

Introduction

Collagen and chitosan are widely recognized as natural biomaterials with great potential in pharmaceutical and biomedical applications because they are biocompatible, biodegradable, and able to support tissue regeneration [1,2]. Collagen forms strong and stable fibrillar structures, making it essential in products such as wound dressings [3], drug delivery systems, and tissue substitutes [4,5]. Across the past few decades, the collagen industry has relied heavily on bovine and porcine derivatives as its main raw material sources. However, growing concerns about biological

safety, environmental impact, and ethical or religious acceptability have encouraged researchers to explore safer and more sustainable alternatives. Spanish skin, a readily available by-product from local fish-processing activities, has emerged as a promising option due to its relatively small molecular size, good absorption characteristics [6], and reported biofunctional properties suitable for medical use [7,8].

South Kalimantan is known for its amplang-processing industry. This industry produces a significant amount of Spanish mackerel skin as a by-product, but its utilization remains limited to products such as dried skin or fish crackers [9]. Several studies have also explored dried Spanish mackerel skin as a source of hydrolyzed collagen for food and cosmetic applications [6,10]. In addition, coastal areas of Kalimantan are major producers of frozen blue crab for export, generating large quantities of shell by-products. These shells are rich in chitin, which can be converted into chitosan, a bioactive polymer with antibacterial properties, regenerative activity, and the ability to promote wound healing [11,12]. The combination of collagen and chitosan in a single composite material may produce synergistic effects: collagen provides a biocompatible structure resembling the tissue matrix, while chitosan offers antibacterial protection and bioactivity needed to prevent infection in wounds [1,2].

Various studies have demonstrated the potential of collagen–chitosan composites for biomedical applications [2], including modified formulations designed to enhance material stability, tissue regeneration, and antibacterial activity [13,14]. Nevertheless, most existing research still relies on commercial collagen or collagen derived from terrestrial animals [15,16], raising concerns related to biological safety, sustainability, as well as ethical and halal acceptability. In addition, the chitosan used is generally sourced from commercial raw materials [1,17] and the integrated utilization of local fishery by-products as sources of both biopolymers remains limited. Studies that combine natural material extraction, comprehensive physicochemical characterization, and antibacterial evaluation within a single integrated research framework are also still scarce, particularly those utilizing Indonesian marine resources. Therefore, this study extracts collagen from Spanish mackerel skin and chitosan from blue swimming crab shells, formulates them into a collagen–chitosan composite, and systematically evaluates their structural, chemical, and antibacterial properties as a sustainable marine-based biomaterial candidate for wound dressing applications.

Materials and methods

Materials

The materials used in this study consisted of primary raw materials and supplementary reagents. The primary raw material was by-product Spanish mackerel (*Scomberomorus commerson*) skin and Blue Swimming Crab (*Portunus pelagicus*) shell, obtained from MSMEs (Micro, Small, and Medium Enterprises) in South Kalimantan. The supplementary reagents included distilled water, technical-grade sodium hydroxide (NaOH), technical-grade acetic acid (CH_3COOH), hydrochloric acid (HCl), sodium chloride (NaCl), butyl alcohol and strain bacteria *Escherichia coli* (ATCC 25922), and *Staphylococcus aureus* (ATCC 29213). The equipment employed was divided into extraction and analytical instruments. The extraction stage utilized an analytical balance (OHAUS), a beaker glass 2L, plastic wrap, thermometer, nylon mesh 100 mesh, pH indicator paper, pH meter, showcase, UV-Vis Spectrophotometer (Thermo Scientific Orion AquaMate 8100), centrifuge (Infitek), and freeze dryer (Daihan Scientific, FD-10N-60A, Maskot). For analysis, the instruments included a pH meter, oven (Thermo Scientific Heratherm OGS100), Fourier Transform Infrared Spectrometer (FTIR) (FTIR with Eco-ATR, Bruker & Confocal Laser Raman Spectrometer HO-SP-CRM216), and Scanning Electron Microscope-Energy Dispersive X-Ray (SEM-EDX) (SEM Evo 10 Carl Zeiss, with EDX).

Acid-Soluble Collagen (ASC) and chitosan extractions

Spanish mackerel skin was subjected to an extraction procedure adapted and modified from a previously reported method [18]. The skin was cleaned, cut into approximately 1 cm^2 pieces, and stored at −20 °C prior to use. Pretreatment involved alkaline treatment (0.1 M NaOH, 1:10 w/v, 4 °C, 12 h; solution renewed every 2 h) to remove non-collagenous proteins, followed by defatting using 10 %(v/v) butyl alcohol (1:10 w/v, 48 h). After washing to neutral pH, acid hydrolysis was carried out with 0.5 M acetic acid (1:15 w/v) at 4 °C for 72 h with periodic stirring. The extract was filtered to

remove insoluble residues, and collagen was precipitated by salting-out with 1.8 M NaCl and collected by centrifugation. The precipitate was redissolved in 0.3 M acetic acid (1:2 w/v) and dialyzed using a 14 kDa molecular weight cut-off membrane against acetic acid and distilled water. The extraction process produced acid-soluble collagen (ASC), which was subsequently freeze-dried prior to characterization. All experiments were conducted in triplicate.

Chitosan was prepared from blue swimming crab shells according to previously reported procedures with minor adjustments [19]. The shells were cleaned, dried, milled, and sieved (100 mesh). Demineralization was performed using 7% HCl (1:7 w/v, 90 °C, 2 h), followed by deproteinization with 8% NaOH (1:10 w/v, 90 °C, 2 h) and deacetylation using 50% NaOH (1:10 w/v, 140 °C, 2 h). Between each step, samples were washed to neutral pH under continuous stirring. The resulting chitosan was dried at 40 °C for 8 h and stored in airtight containers for subsequent characterization. All treatments were performed in triplicate.

Analysis of soluble protein concentration

Protein concentration was determined using the [20] with bovine serum albumin (BSA) as the calibration standard. Absorbance was measured at 595 nm using a UV-Vis spectrophotometer, and protein concentrations were calculated from a BSA standard curve. All measurements were performed in triplicate.

Degree of swelling

The swelling degree was assessed to examine the effect of acetic acid (CH_3COOH) immersion time on the Spanish mackerel's skin. Acetic acid causes the skin to swell, facilitating extraction. The swelling degree (%) was calculated according to [21], as expressed by the following equation:

$$Degree\ of\ Swelling\ (\%) = \frac{W_2 - W_1}{W_1} \text{ x } 100\% \qquad (1)$$

where, W_1 represents the sample weight before immersion, and W_2 represents the sample weight after immersion.

Yield measurement

Collagen yield was determined by comparing the weight of collagen obtained to the initial weight of the skin raw material [22]. The yield was calculated using the following formula:

$$Collagen\ Yield\ (\%) = \frac{Weight\ of\ Collagen\ (g)}{Weight\ of\ Raw\ Material\ (g)} \text{ x } 100 \qquad (2)$$

Degree of deacetylation

The degree of deacetylation (DD) of chitosan was determined by potentiometric titration following standard procedures, with calculation adapted [23]. Chitosan samples were dissolved in 0.1 M HCl under continuous stirring to ensure complete protonation of amino groups. The solution was then titrated with 0.1 M NaOH while monitoring pH changes to obtain the titration curve. The DD value was derived from the quantitative relationship between free amino groups and acetylated units, which reflects the chemical reactivity and functional performance of chitosan. In addition to titration, the DD calculation was supported by FTIR analysis using the absorption ratio between 1,320 and 1,420 cm^{-1} according to the Brugnerotto equation:

$$DA\ (\%) = \frac{A1320}{A140} - \frac{0.3822}{0.03133)}$$
$$DD\ (\%) = 100 - DA \qquad (3)$$

where A_{1320} and A_{1420} are the absorbance values at 1,320 and 1,420 cm^{-1}, respectively.

Proximate analysis

Proximate analysis of fish skin and crab shell samples was performed to determine moisture, ash, lipid, and protein contents according to standard AOAC methods [24]. These parameters were used to assess raw material quality and the effectiveness of the extraction processes. All measurements were conducted in triplicate to ensure accuracy and reproducibility.

SEM-EDX Procedure

The morphological and elemental characteristics of collagen extracted from Spanish mackerel skin and chitosan were observed using Scanning Electron Microscope-Energy Dispersive X-Ray (SEM-EDX) (SEM Evo 10 Carl Zeiss, with EDX), following previously reported methods with minor modifications

[25]. Freeze-dried collagen and powdered chitosan samples were mounted on aluminum stubs with double-sided carbon tape and coated with a thin layer of gold to enhance conductivity. Surface morphology was examined under high vacuum, and EDX spectra were collected to identify elemental composition. The analysis focused on carbon and oxygen as the predominant elements in collagen, whereas carbon, oxygen, calcium, magnesium, and phosphorus were identified as the main constituents in chitosan.

FTIR Procedure

The functional groups of collagen extracted from Spanish mackerel skin and chitosan from crab shells were analyzed by Fourier Transform Infrared Spectroscopy (FTIR with Eco-ATR, Bruker & Confocal Laser Raman Spectrometer HO-SP-CRM216), based on established methods with minor adjustments [26]. Dried samples were finely ground and homogenized with potassium bromide (KBr) to form transparent pellets. Spectra were recorded in the range of 4,000 - 400 cm^{-1} with a resolution of 4 cm^{-1}. The absorption bands were examined to identify functional groups and confirm the structural characteristics of collagen and chitosan.

Antibacterial assay

The antibacterial activity was evaluated using the agar diffusion method with slight modifications based on previously reported procedure [1,27]. A 20 mL nutrient agar plate was inverted and dried at 37 °C for 30 min to obtain a solid nutrient agar plate. Approximately 0.5 mg of chitosan and formulation (chitosan + collagen) samples were pipetted into the wells prepared on the agar plate. The test bacteria used in this study were *Escherichia coli* and *Staphylococcus aureus*. The agar plate was incubated overnight at 37 °C. The diameter of the zone of inhibition that appeared on the surface was measured in 5 directions. The average value was used to calculate the zone of inhibition (ZoI).

Data analysis

The results were analyzed using ANOVA and continued with the Tukey test. The difference was used to optimize the NaOH soaking pretreatment process for making ASC by looking at the concentration of dissolved protein.

Results and discussion

The proximate compositions of Spanish mackerel skin

The raw materials for ASC extraction were from Spanish mackerel skin. The materials were analyzed for proximate composition, including moisture, ash, protein, lipid, and carbohydrate contents (**Table 1**). The proximate composition of raw materials plays an important role in determining extraction efficiency and the quality of the resulting collagen [28]. The data reflect the characteristics of the dermal matrix, providing a baseline for collagen extraction.

Table 1 Proximate composition of Spanish mackerel skin.

Raw material	Moisture	Ash	Protein	Lipid
Spanish Mackerel skin (ww %)	67.59 ± 0.61	0.72 ± 0.09	25.98 ± 0.07	3.92 ± 0.09

Note: Values are expressed as mean ± standard deviation (n = 3).

In this study, Spanish mackerel skin contained 25.98% protein, slightly higher than the 23.13% reported previously [29] and within the 20% - 29.07% range documented for other fish species such as Pangasius, Red Tilapia, Red Snapper, Parrotfish, and Ganglomo [30]. This finding highlights the competitive potential of mackerel skin as a collagen source, further supported by its abundance in Indonesian waters. High protein content reflects the substantial availability of collagen within the dermal matrix [31], whereas relatively low lipid and ash contents support a more efficient extraction process [32]. Excessive lipid content can hinder acid penetration into collagen tissues and reduce extraction efficiency, while high mineral content may interfere with collagen solubility and purity [33,34]. Therefore, an appropriate raw material composition can result in higher collagen yield and improved purity. High-quality collagen is essential for subsequent formulation stages, as its purity and structural integrity influence the stability and

homogeneity of interactions with chitosan during composite formation [35].

Soluble protein concentration after pre-treatment with 0.1 M NaOH Immersion

Pre-treatment of Spanish mackerel skin with 0.1 M NaOH was proven effective in removing non-collagenous proteins, pigments, and other impurities from the dermal matrix [36]. The concentration of soluble protein decreased with immersion time, stabilizing after 8 h, consistent with the result of research [10]. Residual NaOH solutions after immersion at different time intervals (2 - 12 h) confirmed this trend (**Figure 1**). This pattern indicates a shift from rapid protein removal to a plateau, suggesting reduced efficiency as easily extractable components become limited. The slight increase at prolonged immersion (10–12 h) may indicate reduced process selectivity under extended alkaline exposure.

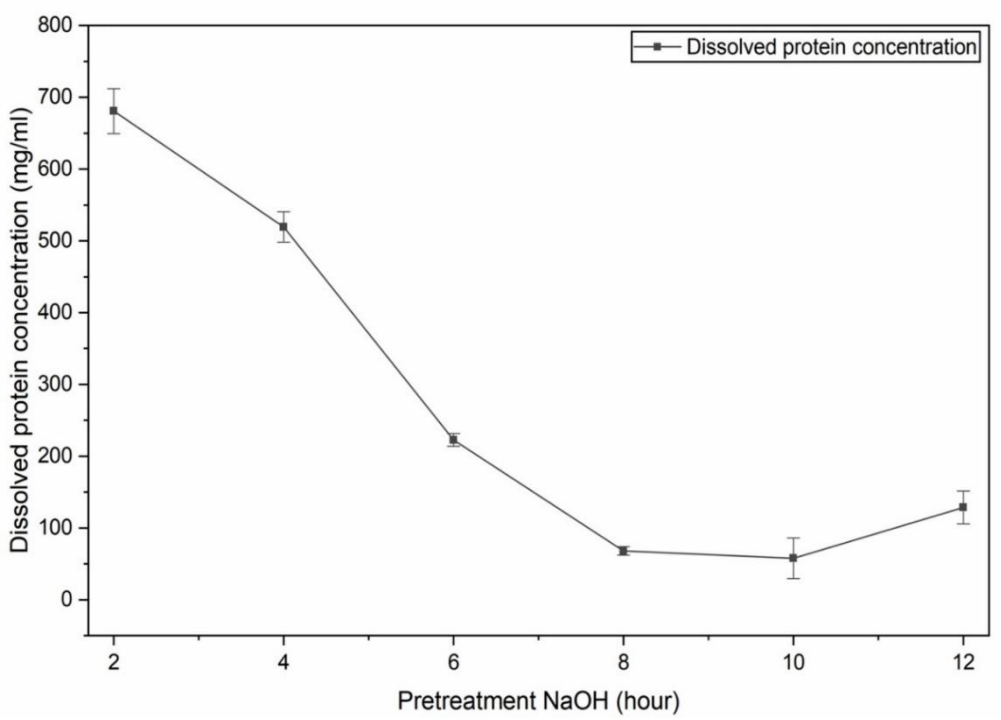

Figure 1 Dissolved protein concentration after 0.1 M NaOH pre-treatment (Mean ± SD; $n = 3$).

The results indicate that most non-collagenous proteins were eliminated before 8 h of treatment, thereby improving the initial purity of collagen and enhancing the quality of the raw material for subsequent extraction stages. Insufficient deproteinization allows residual non-collagen proteins to reduce collagen purity and interfere with the isolation process, resulting in lower yield and poorer structural quality of the extracted collagen [37]. Collagen with low purity may exhibit reduced stability and suboptimal functional properties [38] and may also disrupt the interaction between collagen and chitosan during composite formation. These findings are consistent with previous reports indicating that controlled alkaline treatment can effectively remove proteins and pigments while preserving the triple-helix structure of collagen [39], whereas excessive treatment may lead to partial denaturation and decreased yield due to structural degradation [40,41]. Therefore, the stabilization of protein concentration after 8 h indicates the attainment of optimal conditions between effective non-collagen protein removal and preservation of collagen integrity, which is essential for obtaining collagen with adequate purity, yield, and stability for biomaterial applications.

Swelling of fish skin during pre-treatment

Following optimal pre-treatment (8 h NaOH immersion), the skin was hydrolyzed with 0.5 M acetic acid for 3 days, resulting in 386 ± 12.5% swelling (**Figure 2**). Visually, the untreated skin appeared dense, dry, and tightly packed, whereas after acid treatment the structure became more translucent, swollen, and

partially separated, indicating increased water uptake and matrix relaxation. The obtained value indicates substantial hydration of the collagen matrix, which enhances acid penetration and improves collagen solubilization efficiency through increased interfibrillar spacing and weakening of intermolecular interactions [41]. The observed swelling degree falls within the typical range reported for fish skin collagen raw materials (150% - 600%) [32,42], suggesting sufficient matrix expansion without excessive structural degradation. Optimal swelling contributes to improved collagen yield and purity by facilitating more efficient solvent diffusion, whereas insufficient or excessive swelling may reduce extraction efficiency and damage collagen structure [43]. Therefore, the swelling value obtained reflects extraction conditions that are both efficient and capable of preserving the structural integrity of collagen for biomaterial applications.

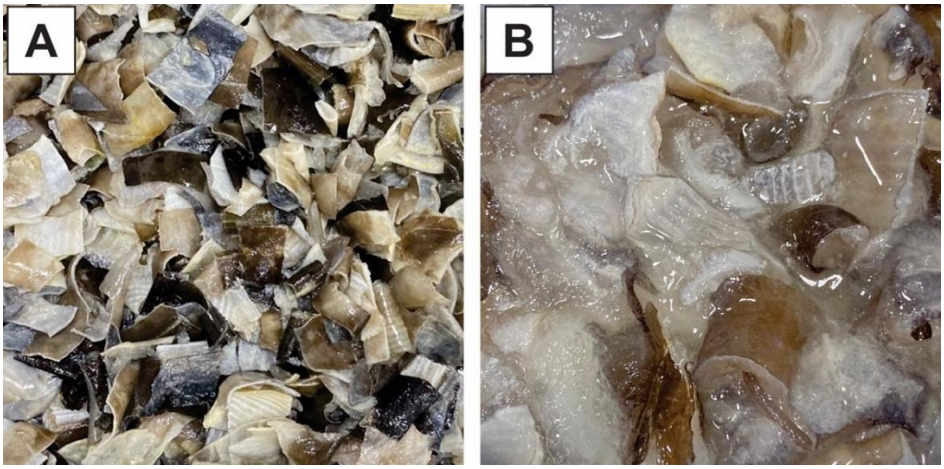

Figure 2 Mackerel skin before acetic acid immersion (A) and after acetic acid immersion (B).

The filtrate obtained after hydrolysis in the acidic solution was subsequently freeze-dried to produce dry collagen. This process preserved collagen structural integrity while yielding a stable porous product suitable for further characterization and biomaterial applications. The dried structure exhibits a porous morphology, indicating effective water sublimation and the formation of a stable matrix for further characterization.

Morphological and yield characteristics of ASC

Morphological differences between ASC before and after freeze-drying are shown in **Figure 3**. Initially, ASC appeared as a soft yellowish gel (A), which transformed into a porous white solid after freeze-drying (B). This transformation reflects successful water removal by sublimation, yielding collagen with improved stability and ease of application.

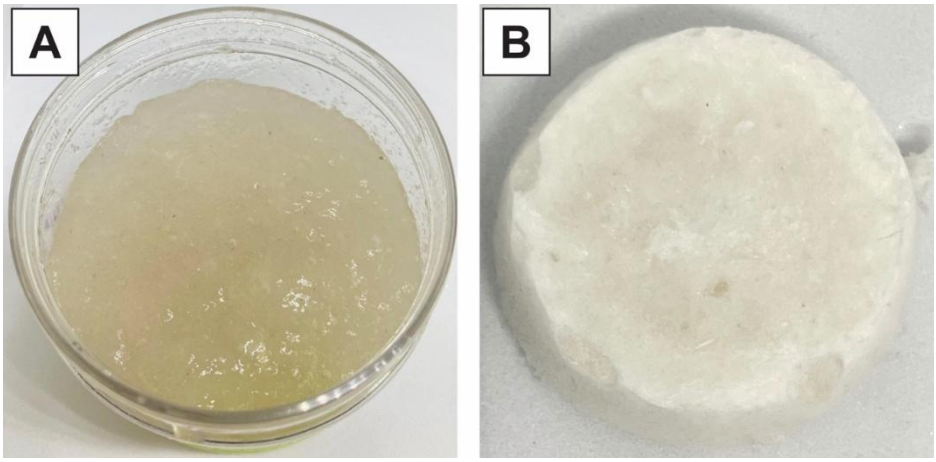

Figure 3 Acid-soluble collagen (ASC) before freeze-drying (A) and following freeze-drying (B).

The obtained ASC showed a yield of 3.125 ± 1.45%, which falls within the typical range of acid-soluble collagen yields reported from various fish skins, such as needlefish and bigeye tuna (3.05%) [41,44]. and catfish (9.3%) [45]. These variations in yield are generally influenced by the protein content of the raw material and extraction conditions, including the duration of acid immersion or hydrolysis [32,44]. Nevertheless, the high swelling degree observed in this study indicates sufficient matrix expansion to support extraction efficiency and produce ASC suitable for biomaterial development.

Characterization of ASC through SEM–EDX and FTIR analyses

SEM–EDX analysis was conducted to evaluate the structural and compositional changes occurring during the collagen extraction process in Spanish mackerel skin and the resulting freeze-dried ASC. The comparative findings for both samples are presented in **Figure 4**.

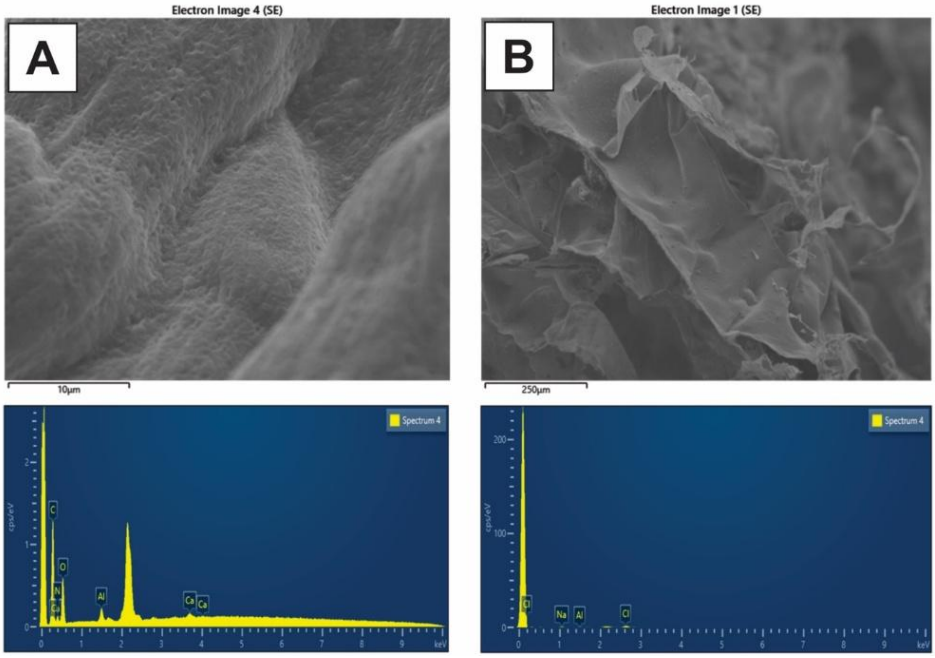

Figure 4 SEM-EDX analysis of Spanish mackerel skin (A) and ASC after freeze-drying (B).

SEM observations revealed a clear morphological transition from the dense and compact structure of Spanish mackerel skin to a more porous and fibrillar ASC structure after acid extraction and freeze-drying, consistent with several previous studies [45,46]. This transition indicates that non-collagenous components were effectively removed and collagen fibrils were successfully separated from the original dermal matrix [45]. The resulting fibrillar structure exhibited a relatively organized and interwoven arrangement, reflecting preservation of collagen integrity and the formation of a porous microstructure that facilitates fluid and oxygen diffusion. EDX analysis consistently confirmed a reduction in mineral content after the extraction process. Raw fish skin generally contained detectable inorganic elements such as calcium and sodium. However, the purified extracted collagen was dominated by carbon (C) and oxygen (O), with a significant decrease in mineral peaks [46]. This finding indicates the effectiveness of demineralization and deproteinization processes in improving collagen purity [47]. The reduction of inorganic residues plays an important role in producing collagen with better structural homogeneity and enhancing its stability and compatibility for biomedical applications [48].

The FTIR spectrum of ASC exhibited characteristic collagen absorption bands (**Figure 5**), with major peaks observed at 3,345 cm^{-1} (N–H, amide A), 2,924 - 2,853 cm^{-1} (aliphatic C–H), 1,654 cm^{-1} (C=O, amide I), 1,545 cm^{-1} (N–H/C–N, amide II), and 1,240 cm^{-1} (C–N/N–H, amide III), confirming the presence of type I collagen [49,50]. The clear presence of amide I–III bands indicates that the triple-helix structure of collagen was preserved during the

extraction and freeze-drying processes [51]. The stability of this triple-helix structure is a key indicator of collagen quality, as it is closely related to thermal stability, mechanical properties, and suitability for biomaterial applications, particularly as a supporting matrix in wound dressing systems [52].

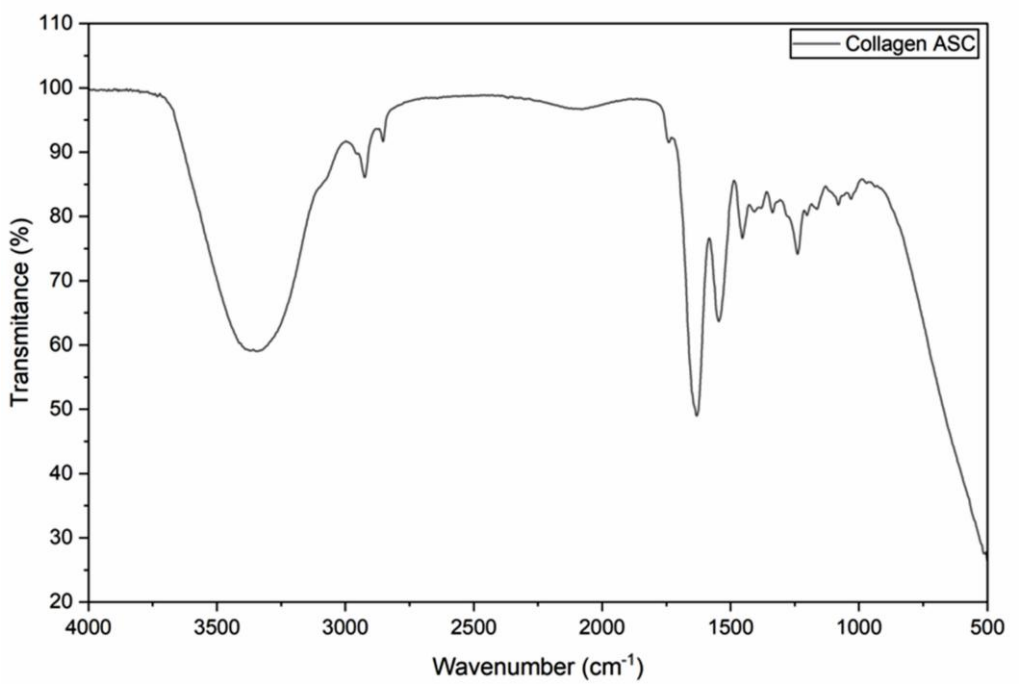

Figure 5 FTIR spectrum of ASC extracted from spanisch mackerel skin after freeze-drying.

Compositional changes and physicochemical properties of extracted chitosan

The extraction of blue swimming crab shells into chitosan (**Table 2**) confirms the effective implementation of demineralization and deproteinization as essential steps in chitosan formation [53,54]. Ash content showed no significant difference between the raw material and chitosan after demineralization, indicating that residual mineral fractions may still influence the solubility and viscosity of the resulting chitosan [55]. In contrast, protein content showed a significant reduction, indicating the effectiveness of the deproteinization process in removing non-chitin proteins, thereby enhancing the purity of the chitin matrix and supporting a more optimal deacetylation process [56]. This condition is consistent with previous studies reporting that the removal of proteins and minerals from crustacean shells is a critical factor in producing chitosan with a more homogeneous polymer structure [57].

Table 2 Characteristics of raw materials and chitosan extracted from blue swimming crab shells.

Parameter	Raw material	Chitosan
Appearance	Powder	Powder
Moisture (%)	1.58 ± 0.05^{a}	1.57 ± 0.05^{a}
Ash (%)	73.61 ± 0.26^{a}	73.49 ± 0.17^{a}
Crude protein (%)	12.56 ± 0.13^{a}	7.48 ± 0.04^{b}
Lipid (%)	0.39 ± 0.30^{a}	0.07 ± 0.06^{b}
Yield (%)	-	19.06 ± 0.32
Viscosity (mPa·s)	-	65.3 ± 2.08

Note: Values are expressed as mean ± standard deviation (n = 3). Different superscript letters within the same parameter indicate significant differences between raw material and extracted chitosan ($p < 0.05$).

The data further indicate a consistent reduction in lipid content alongside stable moisture levels, suggesting improved material stability and reduced interference from residual components in the extracted chitosan. The obtained chitosan yield falls within the general range reported for crustacean-based chitosan in previous studies, typically around 5% - 50% [58-60], indicating efficient conversion of chitin into chitosan without excessive polymer degradation. Moreover, the viscosity of crustacean-derived chitosan, which generally ranges from 20 - 200 mPa·s [61,62], reflects adequate polymer chain length for film formation and stable composite structure development. The combination of improved purity, optimal yield, and suitable viscosity, in agreement with previous studies, confirms that chitosan derived from blue swimming crab shells possesses appropriate physicochemical properties for biomaterial applications, particularly as a matrix in collagen–chitosan composite formulations.

Morphological and elemental characterization of raw crab shell and extracted chitosan (SEM–EDX)

The SEM–EDX results in **Figure 6** show structural and chemical compositional changes following the extraction of chitosan from blue swimming crab shells, consistent with the characteristics presented in **Table 2**. The raw shells exhibited a dense structure dominated by a mineral–protein–chitin complex, particularly calcium carbonate, as previously reported in crustacean shell matrices [63,64]. Calcium carbonate is strongly bound to the chitin matrix and is reflected by the dominant presence of Ca, Mg, and P elements in the EDX spectrum. After the demineralization and deproteinization processes, the chitosan surface became smoother and more homogeneous, similar to observations reported for the same species despite differences in extraction temperature and duration [65].

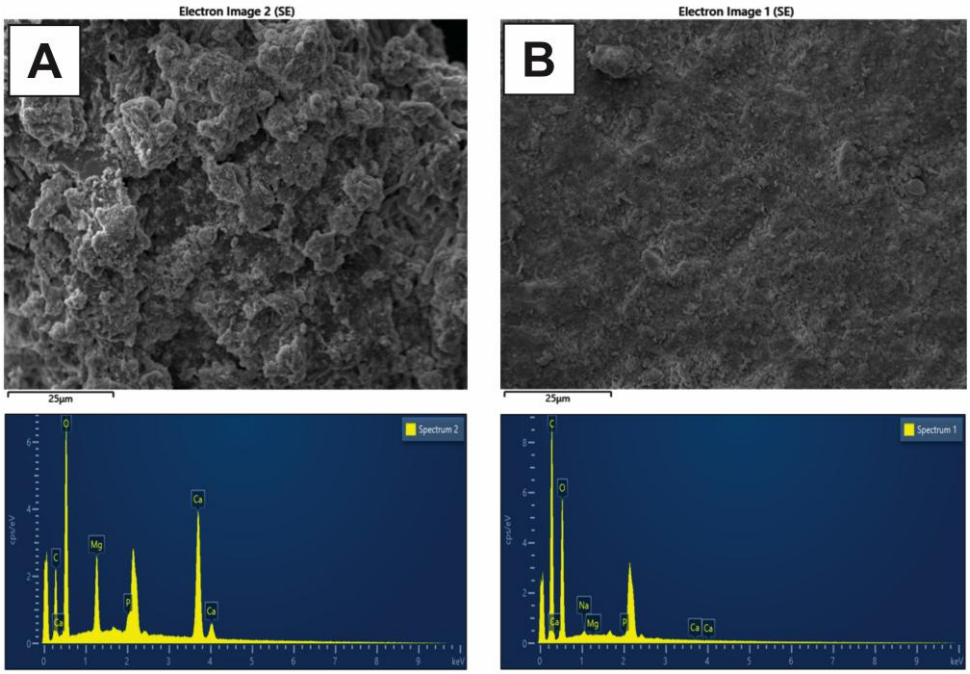

Figure 6 SEM micrographs of blue swimming crab shells (A) chitosan blue swimming crab (B).

The reduction in mineral element intensity and the dominance of C and O in the EDX spectrum indicate the removal of mineral and protein components from the chitin matrix and the formation of a characteristic polysaccharide structure of chitosan [66]. These findings are consistent with the results presented in **Table 2**, which show that most structural proteins associated with chitin were hydrolyzed and solubilized during alkaline treatment, thereby increasing the purity of the chitin matrix and facilitating the removal of acetyl groups during the deacetylation process. This condition

contributed to the formation of a smoother and more homogeneous chitosan morphology.

Functional group profiles and degree of deacetylation analysis

The FTIR spectra presented in **Figure 7** demonstrate distinct differences in functional group characteristics among blue swimming crab (BC) chitosan, commercial chitosan, and the raw crab shell material, supporting the structural and compositional changes previously observed in the SEM–EDX analysis and the physicochemical characteristics. A broad absorption band in the range of 3,100 + 3,500 cm^{-1}, associated with –OH and –NH stretching vibrations, appears more intense in BC chitosan, indicating a higher degree of deacetylation and an increased number of free amine groups [67]. The Amide I band, typically located at 1,620 - 1,655 cm^{-1}, shows lower intensity in BC chitosan compared with the raw material and commercial chitosan, indicating a more efficient deacetylation process. This finding is consistent with the reduction in protein content and the increased purity of the chitin matrix observed in **Table 2**. The spectra also reveal distinct variations in peak distribution and intensity patterns among the samples, reflecting differences in molecular structure and chemical composition following the extraction process.

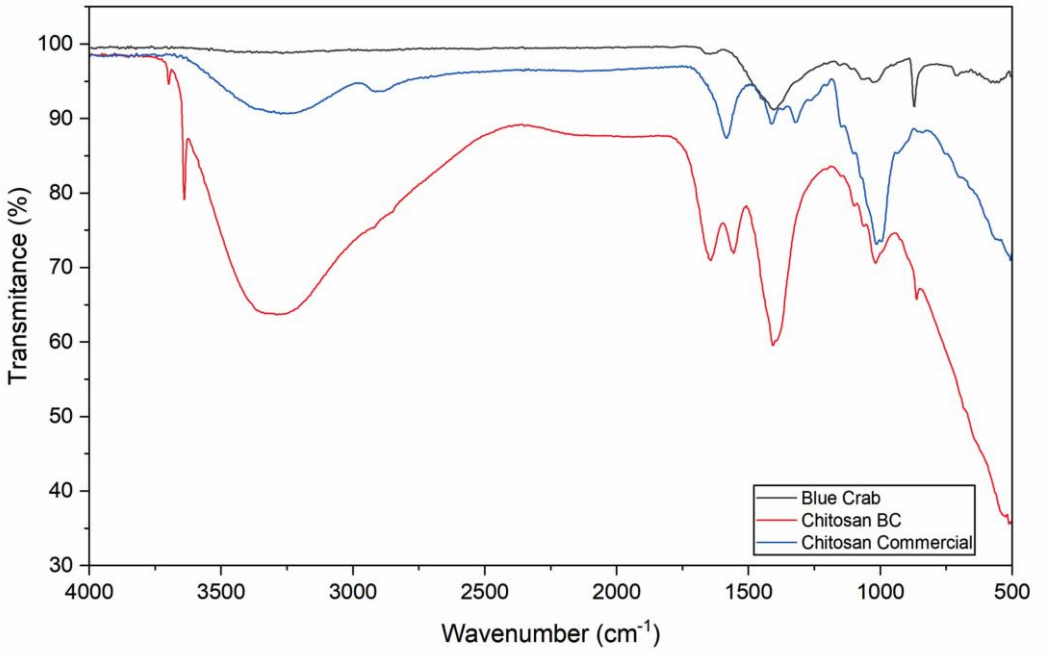

Figure 7 FTIR spectra of blue swimming crab, chitosan blue swimming crab shells and commercial chitosan.

The calculated degree of deacetylation (DD) indicates that BC chitosan achieved a DD value of 92.57%, which is higher than that of commercial chitosan. This value remains within the range reported in previous studies [60,68], typically between 70% and 97.8% for crab shell–based chitosan, depending on extraction methods and deacetylation conditions. A high DD reflects the dominance of free amine groups ($–NH_2$), which contribute to improved solubility [69], enhanced film-forming ability [12], and increased cationic charge of chitosan [70]. These properties promote stronger interactions with negatively charged bacterial cell walls and consequently enhance antibacterial potential [71,72].

Collagen-Chitosan antibacterial assay

Antibacterial activity testing was performed to evaluate the functional potential of BC chitosan and its interaction with ASC collagen within the composite system (**Table 3**). Pure BC chitosan exhibited greater antibacterial activity compared with the collagen–chitosan composite formulations, whereas the blended formulations showed reduced inhibition against *E. coli* and no detectable activity against *S. aureus*. The

antibacterial activity observed for BC chitosan remained within the moderate to strong range [2] commonly reported for crab shell–derived chitosan, approximately 4 - 25 mm, which is influenced by the degree of deacetylation [73] and chitosan concentration [19,74,75]. However, this activity decreased following incorporation with collagen, likely due to a reduction in the effective chitosan concentration and the formation of a denser composite network [1,2]. The data further indicate that variations in the collagen–chitosan ratio do not result in statistically significant differences in inhibition zone diameters, suggesting a limited contribution of compositional variation to antibacterial performance.

Table 3 Inhibition zone of chitosan and chitosan–collagen formulations against *E. coli* and *S. aureus.*

Sample	Inhibition zone diameter (mm)	
	E.coli	***S.aureus***
Control (+)	31.27 ± 0.47^{a}	28.87 ± 0.87^{a}
Control (-)	2.47 ± 0.25^{e}	0^{c}
Col	8.00 ± 0.72^{d}	0^{c}
Ch	18.23 ± 0.20^{b}	15.80 ± 1.65^{b}
Col:Ch (1:1)	15.63 ± 0.25^{c}	0^{c}
Col:Ch (2:1)	16.93 ± 1.04^{c}	0^{c}
Col:Ch (1:2)	16.33 ± 0.55^{c}	0^{c}

Note: Values are presented as mean ± standard deviation (n = 3). Different superscript letters within the same column indicate significant differences between samples ($p < 0.05$).

The antibacterial properties of chitosan are closely associated with the presence of positively charged free amine groups ($–NH_2$), which interact electrostatically with negatively charged bacterial cell surfaces. These interactions disrupt membrane permeability and inhibit bacterial growth [76]. The results indicate that *E. coli* was more susceptible than *S. aureus*, which can be attributed to differences in cell wall structure [77]. Gram-negative bacteria such as *E. coli* possess a thinner peptidoglycan layer [78,79], facilitating interaction with chitosan, whereas Gram-positive bacteria such as *S. aureus* have a thicker peptidoglycan layer that restricts chitosan penetration [74,80]. Within the collagen–chitosan composite system, partial interaction between chitosan amine groups and collagen reduces the availability of free amine groups for direct interaction with bacterial cells.

Interactions between ASC collagen and BC chitosan primarily occur through hydrogen bonding between the hydroxyl and carboxyl groups of collagen and the amine groups of chitosan, leading to the formation of a more compact and interconnected polymer network [81]. The establishment of this network contributes to improved structural stability and homogeneity of the composite matrix. However, the formation of a dense polymeric structure may also limit the mobility and diffusion of chitosan within the matrix and toward the bacterial surface [78]. As a result, the enhancement of antibacterial activity in the composite formulations remains limited, since a portion of the reactive chitosan groups becomes involved in internal network formation rather than interacting directly with bacterial cells. Similar observations have been reported in previous studies, where strong intermolecular interactions within collagen–chitosan systems reduced the availability of active functional groups responsible for antibacterial performance [13,78,82]. Therefore, optimizing the proportion of chitosan within the composite or incorporating additional antibacterial agents may enhance antibacterial effectiveness while maintaining the structural integrity of the collagen–chitosan biomaterial [15].

Conclusions

This study demonstrates that collagen and chitosan can be successfully obtained from Spanish mackerel skin and blue swimming crab shells while preserving their essential structural and functional characteristics.

SEM–EDX and FTIR analyses confirmed effective purification and the presence of key functional groups, while antibacterial evaluation indicated that antimicrobial activity was primarily attributed to chitosan, with limited synergistic effects observed in collagen–chitosan composite formulations. These findings highlight the potential of fishery by-products as sustainable sources of biomaterials for wound dressing applications. However, the reduced antibacterial performance in composite formulations indicates that optimizing the proportion of chitosan within the matrix is essential to maintain the availability of active functional groups. The incorporation of additional antibacterial agents may further enhance antimicrobial effectiveness without compromising the structural integrity of the collagen–chitosan biomaterial. Therefore, future studies should focus on formulation optimization and systematic *in vitro* evaluation prior to advanced functional testing and *in vivo* validation to strengthen their biomedical and therapeutic relevance.

Acknowledgements

Support for this research was obtained from the Ministry of Higher Education, Science, and Technology of Indonesia through the Basic Research Scheme No. 075/C3/DT.05.00/PL/2025. The authors gratefully acknowledge this funding.

Declaration of Generative AI in Scientific Writing

The authors utilized generative AI tools (such as QuillBot and OpenAI's ChatGPT) solely to assist with language refinement and grammatical improvements during manuscript preparation. No sections of the scientific content, analysis, or data interpretation were generated by AI. All authors retain complete responsibility for the accuracy, integrity, and conclusions presented in this work.

CRediT Author Statement

Sitti Hardiyanti Rachman: Conceptualization; Methodology; Data Curation; Writing - Original Draft. **Mila Safitri Rizfa:** Formal analysis; Resources; Writing - Review & Editing, **Shanca Kusumo:** Investigation; Methodology. **Syarifah Nafhastus Sehroh:** Investigation; Methodology; **Iskarimah Atqiah:** Investigation; Methodology. **Rachmat Hidayat:** Visualization data and Investigation. **Fahri Sinulingga:** Writing, reviewing and editing manuscript. All authors have read and agreed to the published version of the manuscript.

References

[1] RD Valenzuela-Rojo, J López-Cervantes, DI Sánchez-Machado, AA Escárcega-Galaz and MDR Martínez-Macias. Antibacterial, mechanical and physical properties of collagen - chitosan sponges from aquatic source. *Sustainable Sustainable Chemistry and Pharmacy* 2020; **15**, 100218.

[2] MP Pimenta, N Fernández, ARC Duarte, R Bronze, J Marto and FB Gaspar. Collagen–chitosan composites enhanced with hydroxytyrosol for prospective wound healing uses. *Pharmaceutics* 2025; **17**, 618.

[3] S Sharma, V Kumar, RK Narang and TS Markandeywar. Collagen-based formulations for wound healing: A literature review. *Life Sciences* 2022; **290**, 120096.

[4] M Furtado, L Chen, Z Chen, A Chen and W Cui. Development of fish collagen in tissue regeneration and drug delivery. *Engineered Regeneration* 2022; **3(3)**, 217-231.

[5] KS Silvipriya, KK Kumar, AR Bhat, BD Kumar and A John. Collagen: Animal sources and biomedical application. *Journal of Applied Pharmaceutical Science* 2015; **5(3)**, 123-127.

[6] CF Chi, ZH Cao, B Wang, FY Hu, ZR Li and B Zhang. Antioxidant and functional properties of collagen hydrolysates from Spanish mackerel skin as influenced by average molecular weight. *Molecules* 2015; **19(8)**, 11211-11230.

[7] JB Zhang, YQ Zhao, YM Wang, CF Chi and B Wang. Eight collagen peptides from hydrolysate fraction of Spanish mackerel skins: Isolation, identification, and *in vitro* antioxidant activity evaluation. *Marine Drugs* 2019; **17(4)**, 224.

[8] ZR Li, B Wang, CF Chi, QH Zhang, YD Gong, JJ Tang, HY Luo and GF Ding. Isolation and characterization of acid-soluble and pepsin-soluble collagens from the skin and bone of Spanish mackerel (*Scomberomorus niphonius*). *Food Hydrocolloids* 2013; **31(1)**, 103-113.

[9] P Purnomo and J Suhanda. Long time curing process of Spanish mackerel skin

(*Scomberomorus commersonii*) as raw material. *Fish Scientiae* 2017; **7(1)**, 83.

[10] H Rahmawati, TW Agustini, EN Dewi and A Trianto. Characteristics of Spanish mackerel dry skin collagen hydrolysate with papain enzyme. *Jurnal Pengolahan Hasil Perikanan Indonesia* 2024; **27(12)**, 1156-1171.

[11] MA Matica, FL Aachmann, A Tøndervik, H Sletta and V Ostafe. Chitosan as a wound dressing starting material: Antimicrobial properties and mode of action. *International Journal of Molecular Sciences* 2019; **20(23)**, 5889.

[12] I Aranaz, AR Alcántara, MC Civera, C Arias, B Elorza, AH Caballero and N Acosta. Chitosan: An overview of its properties and applications. *Polymers* 2021; **13(19)**, 3256.

[13] H Xie, X Chen, X Shen, Y He, W Chen, Q Luo, W Ge, W Yuan, X Tang, D Hou, D Jiang, Q Wang, Y Liu, Q Liu and K Li. Preparation of chitosan–collagen–alginate composite dressing and its promoting effects on wound healing. *International Journal of Biological Macromolecules* 2017; **107**, 93-104.

[14] N Naghshineh, K Tahvildari and M Nozari. Preparation of chitosan, sodium alginate, gelatin and collagen biodegradable sponge composites and their application in wound healing and curcumin delivery. *Journal of Polymers and the Environment* 2019; **27**, 2819-2830.

[15] A Sionkowska and K Musiał. Fish collagen and chitosan mixtures as a promising biomaterial for potential use in medicine and engineering of biomaterials. *Engineering of Biomaterials* 2022; **164**, 16-24.

[16] A Martínez, MD Blanco, N Davidenko and RE Cameron. Tailoring chitosan/collagen scaffolds for tissue engineering: Effect of composition and different crosslinking agents on scaffold properties. *Carbohydrate Polymers* 2015; **132**, 606-619.

[17] AC Ferreira, MRQ Bomfim, CHBDC Sobrinho, DTL Boaz, RLDS Lira, VC Fontes, MO Arruda, PMW Zago, CAAD Filho, CJM Dias, MOBDR Borges, RM Ribeiro, CWB Bezerra and RS Penha. Characterization, antimicrobial and cytotoxic activity of polymer blends based on chitosan and fish collagen. *AMB Express* 2022; **12(1)**, 102.

[18] J Li, M Wang, Y Qiao, Y Tian, J Liu, S Qin and W Wu. Extraction and characterization of type I collagen from skin of tilapia (*Oreochromis niloticus*) and its potential application in biomedical scaffold material for tissue engineering. *Process Biochemistry* 2018; **74**, 156-163.

[19] N Luthfiyana, S Bija, E Anwar, DR Laksmitawati and GL Rosalinda. Characteristics and activity of chitosan from mud crab shells on acne bacteria: *Staphylococcus aureus*, *S. epidermidis* and *Propionibacterium acnes*. *Biodiversitas* 2022; **23**, 6645-6651.

[20] MM Bradford. A rapid and sensitive method for the quantitation of microgram quantities of protein utilizing the principle of protein–dye binding. *Analytical Biochemistry* 1976; **72**, 248-254.

[21] Widiyanto, Uju, SH Rachman and M Nurilmala. Preliminary study on hydroxyproline content of purple-spotted bigeye (*Priacanthus tayenus*) scaly skin and its gelatin quality. *Tropical Life Sciences Research* 2025; **36(1)**, 93.

[22] AOAC. *Official methods of analysis of AOAC International*. Association of Official Analytical Chemists, Washington DC, 1995.

[23] J Brugnerotto, J Lizardi, FM Goycoolea, W Argüelles-Monal, J Desbrières and M Rinaudo. An infrared investigation in relation with chitin and chitosan characterization. *Polymer* 2001; **42(8)**, 3569-3580.

[24] AOAC. *Official methods of analysis of the Association of Official Analytical Chemistry*. AOAC International, Washington DC, 1995.

[25] E Mirda, R Idroes, K Khairan, TE Tallei, M Ramli, N Earlia, A Maulana, GM Idroes, M Muslem and Z Jalil. Synthesis of chitosan–silver nanoparticle composite spheres and their antimicrobial activities. *Polymers* 2021; **13(22)**, 3990.

[26] PK Jha, C Pokhum, P Soison, KA Techato and C Chawengkijwanich. Comparative study of zinc oxide nanocomposites with different noble metals synthesized by biological method for photocatalytic disinfection of *Escherichia coli* present in hospital wastewater. *Water Science & Technology* 2023; **88(6)**, 1564-1577.

[27] P Basnet, PK Jha, A Gupta and S Chatterjee. Synergistic effect of tea phytochemicals, noble

metals and ZnO nano-photo-composites for combating resistance of bacterial growth. *Journal of Nano Research* 2021; **70**, 53-66.

[28] V Girsang, J Reveny and M Nainggolan. Isolation and characterization of collagen from patin fish skin (*Pangasius* sp.). *Asian Journal of Pharmaceutical Research and Development* 2020; **8(1)**, 47-51.

[39] F Gunawan, P Suptijah and Uju. Extraction and characterization of gelatin from mackerel skin (*Scomberomorus commersonii*) from Bangka Belitung Province. *Jurnal Pengolahan Hasil Perikanan Indonesia* 2017; **20**, 568-581.

[30] M Nurilmala, H Suryamarevita, HH Husein Hizbullah, AM Jacoeb and Y Ochiai. Fish skin as a biomaterial for halal collagen and gelatin. *Saudi Journal of Biological Sciences* 2022; **29(2)**, 1100-1110.

[31] N Muralidharan, RJ Shakila, D Sukumar and G Jeyasekaran. Skin, bone and muscle collagen extraction from the trash fish, leather jacket (*Odonus niger*) and their characterization. *Journal of Food Science and Technology* 2013; **50**, 1106-1113.

[32] P Patmawati, AR Ergion, L Sulmartiwi, S Raseetha, D Nirmala, Y Waiprib and S Wijayanti. Effect of acetic acid pre-treatment on hydro-extraction of water-soluble collagen from skin of Alaska pollock (*Theragra chalcogramma*). *Jurnal Ilmiah Perikanan dan Kelautan* 2023; **15(2)**, 468-477.

[33] E Kuprina, A Yakkola, A Kopylov, M Zashikhin and A Kuznetsova. Development of functional product enriched with collagen hydrolysate from fish processing waste. *E3S Web of Conferences* 2020; **164(3)**, 06026.

[34] K Chantakun, L Chotphruethipong and S Benjakul. Development of hydrolysis and defatting processes for production of low fishy odor hydrolyzed collagen from fatty skin of sockeye salmon (*Oncorhynchus nerka*). *Foods* 2021; **10(10)**, 2257.

[35] M Danu, B Simionescu, C Ibanescu and SA Ibanescu. Dynamic rheological behavior of chitosan/collagen mixtures. *Revista de Chimie* 2020; **71**, 193-200.

[36] S Kendler, A Sasidharan and T Rustad. Extraction of proteinaceous components and biominerals from cold-water fish filleting side streams: A review. *Frontiers in Sustainable Food Systems* 2023; **7**, 1331113.

[37] D Meng, H Tanaka, T Kobayashi, H Hatayama, X Zhang, K Ura, S Yunoki and Y Takagi. Effect of alkaline pretreatment on biochemical characteristics and fibril-forming abilities of type I and II collagens extracted from bester sturgeon by-products. *International Journal of Biological Macromolecules* 2019; **131**, 572-580.

[38] T Nurhayati, N Nurjanah and I Astiana. Characteristics of papain-soluble collagen from redbelly yellowtail fusilier (*Caesio cuning*). *IOP Conference Series: Earth and Environmental Science* 2018; **196**, 012034.

[39] M Rahaman, S Das, S Sahu, A Karmakar and B Debnath. Extraction, isolation and characterization of collagen peptide from fish and recent biological activities of collagen peptides. *Journal of Survey in Fisheries Sciences* 2023; **10**, 1450-1465.

[40] M Meyer. Processing of collagen-based biomaterials and the resulting materials properties. *Biomedical Engineering Online* 2019; **18**, 24.

[41] TT Heng, JY Tey, KS Soon and KK Woo. Utilizing fish skin of ikan belida (*Notopterus lopis*) as a source of collagen: Production and rheological properties. *Marine Drugs* 2022; **20(8)**, 525.

[42] BFD Zaelani, M Safithri, K Tarman, I Setyaningsih and M Meydia. Collagen isolation with acid-soluble method from the skin of red snapper (*Lutjanus* sp.). *IOP Conference Series: Earth and Environmental Science* 2019; **241**, 012033.

[43] SZ Ramle, SNH Oslan, R Shapawi, RAM Mokhtar, WNM Noordin and N Huda. Biochemical characteristics of acid-soluble collagen from food processing by-products of needlefish skin (*Tylosurus acus melanotus*). *Applied Sciences* 2022; **12(24)**, 12695.

[44] L Devita, M Nurilmala, HN Lioe and MT Suhartono. Chemical and antioxidant characteristics of skin-derived collagen obtained by acid–enzymatic hydrolysis of bigeye tuna

(*Thunnus obesus*). *Marine Drugs* 2021; **19(4)**, 222.

[45] S Xu, H Yang, L Shen and G Li. Purity and yield of collagen extracted from southern catfish (*Silurus meridionalis* Chen) skin through improved pretreatment methods. *International Journal of Food Properties* 2017; **20(S1)**, S141-S153.

[46] E Martins, R Fernandes, AL Alves, RO Sousa, RL Reis and TH Silva. Skin by-products of *Reinhardtius hippoglossoides* (Greenland halibut) as an ecosustainable source of marine collagen. *Applied Sciences* 2022; **12(21)**, 11282.

[47] AA Abbas, KA Shakir and MK Walsh. Functional properties of collagen extracted from catfish (*Silurus triostegus*) waste. *Foods* 2022; **11**, 633.

[48] T Maschmeyer, R Luque and M Selva. Upgrading of marine (fish and crustaceans) biowaste for high added-value molecules and bio(nano)-materials. *Chemical Society Reviews* 2020; **49**, 4527-4563.

[49] O Kaewdang, S Benjakul, T Kaewmanee and H Kishimura. Characteristics of collagens from the swim bladders of yellowfin tuna (Thunnus albacares). *Food Chemistry* 2014; **155**, 264-270.

[50] DN Carolina, MH Satari, BP Priosoeryanto, A Susanto, C Sukotjo and RE Kartasasmita. Exploring carp scales (*Cyprinus carpio* L.) as a novel source of collagen for dental use: Extraction and characterization. *Journal of Applied Pharmaceutical Science* 2024; **14**, 204-209.

[51] HH Abd-Elrahman, WAM Omar and HA Elnashar. Characterization of biochemical and optical properties of Nile tilapia (*Oreochromis niloticus*) corneal collagen. *Future Journal of Pharmaceutical Sciences* 2024; **10**, 39.

[52] RO Sousa, E Martins, DN Carvalho, AL Alves, C Oliveira, ARC Duarte, TH Silva and RL Reis. Collagen from Atlantic cod (*Gadus morhua*) skins extracted using CO_2-acidified water with potential application in healthcare. *Journal of Polymer Research* 2020; **27**, 73.

[53] K Periyannan, H Selvaraj, B Subbu, M Pallikondaperumal, P Karuppiah, JR Rajabathar, H Al-Lohedan and S Thangarasu. Green fabrication of chitosan from marine crustaceans and mushroom waste toward sustainable resource utilization. *Green Processing and Synthesis* 2023; **12(1)**, 0093.

[54] R Ismail, DF Fitriyana, AP Bayuseno, Jamari, PY Pradiptya, RC Muhamadin, FW Nugraha, Rusiyanto, A Setiyawan, A Bahatmaka, HN Firmansyah, S Anis, AP Irawan, JP Siregar and T Cionita. Effect of deacetylation temperature on the characterization of chitosan from crab shells as a candidate for organic nanofluids. *Journal of Advanced Research in Fluid Mechanics and Thermal Sciences* 2023; **103**, 55-67.

[55] A Ewais, RA Saber, AG Abdel Ghany, A Sharaf and M Sitohy. High-quality, low-molecular-weight shrimp and crab chitosans obtained by short-time holistic high-power microwave technology. *SN Applied Sciences* 2023; **5**, 365.

[56] RA Salman and NK Zedain. Chitosan sources and extraction: A review. *Kufa Journal of Engineering* 2025; **16**, 615-631.

[57] MA Ibrahim, SM Mostafa and SM Ibrahim. Effect of extraction techniques on properties and economics of chitosan obtained from shrimp shell waste. *Egyptian Journal of Aquatic Biology and Fisheries* 2019; **23**, 138-142.

[58] S Fadlaoui, O El-Asri, L Mohammed, S Ait Sihame, A Omari and M Melhaoui. Isolation and characterization of chitin from shells of the freshwater crab *Potamon algeriense*. *Progress on Chemistry and Application of Chitin and Its Derivatives* 2019; **24**, 23-35.

[59] A Aberoumand and M Hoseinian. Extraction of chitosan from shells of crab (*Liocarcinus vernalis*). *Applied Food Research* 2025; **5(1)**, 100964.

[60] N Luthfiyana, S Bija, CD Nugraeni, MS Lembang, E Anwar, DR Laksmitawati, PW Nusaibah, P Ratrinia and M Mukmainna. Characteristics and antibacterial activity of chitosan nanoparticles from mangrove crab shell (*Scylla* sp.) in Tarakan Waters, North Kalimantan, Indonesia. *Biodiversitas* 2022; **23**, 4018-4025.

[61] MA Razi, R Wakabayashi, M Goto and N Kamiya. Formation and characterization of caseinate–chitosan nanocomplexes for encapsulation of curcumin. *Journal of Chemical Engineering of Japan* 2018; **51**, 445-453.

[62] E Fakhri, H Eslami, P Maroufi, F Pakdel, S Taghizadeh, K Ganbarov, M Yousefi, A Tanomand, B Yousefi, S Mahmoudi and HS Kafil. Chitosan biomaterials application in dentistry. *International Journal of Biological Macromolecules* 2020; **162**, 956-974.

[63] N Alimatul, H Narudin and AH Mahadi. Chitin, chitosan, and submicron-sized chitosan particles prepared from *Scylla serrata* shells. *Materials International* 2020; **2(2)**, 0139-0149.

[64] MRA Hanan, AK Nasution, R Hussain and S Saidin. Fabrication of poly(lactic-co-glycolic acid)/calcium phosphate bone cement composite: Synthesization of calcium phosphate from crab shells. *Jurnal Teknologi* 2018; **80**, 103-109.

[65] G Hao, Y Hu, L Shi, J Chen, A Cui, W Weng and K Osako. Physicochemical characteristics of chitosan from swimming crab (*Portunus trituberculatus*) shells prepared by subcritical water pretreatment. *Scientific Reports* 2021; **11**, 1646.

[66] MM Sundari, A Jegatheesan, R Mohan, MSA Raj, NA Devi, P Ravikumar, M Ayyanar and K Ravichandran. Exploring the bioactive potential of chitosan extracted from *Portunus trituberculatus* crab shell for multifaceted applications: Antioxidant, antidiabetic, anti-inflammatory and cytotoxic activities. *Materials Letters* 2025; **393**, 138581.

[67] RS Dongre. *Chitosan-derived synthetic ion exchangers: Characteristics and applications*. InTech, Houston TX, 2018.

[68] B Li, X Wu, B Bao, R Guo and W Wu. Evaluation of α-chitosan from crab shell and β-chitosan from squid gladius based on biochemical performance. *Applied Sciences* 2021; **11(7)**, 3183.

[69] MMA Elsoud and EM El Kady. Current trends in fungal biosynthesis of chitin and chitosan. *Bulletin of the National Research Centre* 2019; **43**, 59.

[70] M Zhang, W Zhao, Q Fang, X Wang, C Chen, B Shi, B Zheng, S Wang, W Tan and L Wu. Effects of chitosan–collagen dressing on wound healing *in vitro* and *in vivo* assays. *Journal of Applied Biomaterials & Functional Materials* 2021; **19**, 2280800021989698.

[71] IM Helander, E Nurmiaho-Lassila, R Ahvenainen, J Rhoades and S Roller. Chitosan disrupts the barrier properties of the outer membrane of Gram-negative bacteria. *International Journal of Food Microbiology* 2001; **71**, 235-244.

[72] EI Rabea, MET Badawy, CV Stevens, G Smagghe and W Steurbaut. Chitosan as antimicrobial agent: Applications and mode of action. *Biomacromolecules* 2003; **4**, 1457-1465.

[73] MP Batista, M Pimenta, N Fernández, ARC Duarte, R Bronze, J Marto and FB Gaspar. Collagen–chitosan composites enhanced with hydroxytyrosol for prospective wound healing uses. *Pharmaceutics* 2025; **17(5)**, 618.

[74] J Pradhan, B Baisakhi, BK Das, K Jena, S Ananta and D Mohanty. Chitosan extracted from *Portunus sanguinolentus* (three-spot swimming crab) shells: Its physicochemical and biological potentials. *Journal of Environmental Biology* 2025; **46(2)**, 319-328.

[75] C Metin, Y Alparslan and T Baygar. Physicochemical, microstructural and thermal characterization of chitosan from blue crab shell waste and its bioactivity characteristics. *Journal of Polymers and the Environment* 2019; **27(11)**, 2552-2561.

[76] Z Kassim, WNAW Murni, MRM Razak, WSW Omar and SB Adam. Chitosan isolated from horseshoe crab *Tachypleus gigas* from the Malay Peninsula. *Oriental Journal of Chemistry* 2018; **34(2)**, 928-933.

[77] Hartatiek, F Fathurochman, MI Wuriantika, Yudyanto, Masruroh, DJH Santjojo and M Nurhuda. Mechanical, degradation rate, and antibacterial properties of a collagen–chitosan/PVA composite nanofiber. *Materials Research Express* 2023; **10**, 025401.

[78] M Rohde. The Gram-positive bacterial cell wall. *Microbiology Spectrum* 2019; **7(3)**, 10.

[79] B Aragón, L Alberto, J Mejía, L Meza, J Edmundo and P Damián. Composites of silver–chitosan nanoparticles: A potential source for new antimicrobial therapies. *Revista Mexicana de Ciencias Farmacéuticas* 2016; **47(1)**, 7-25.

[80] F Shahidi, VVaratharajan, H Peng and R Senadheera. Utilization of marine by-products for the recovery of value-added products. *Journal of Food Bioactives* 2019; **6(6)**, 10-61.

[81] G Dolete, TM Bianca, O Tutunari, IC Mocanu, C Balas, IL Ardelean, DS Dragan, CM Kamerzan and SS Maier. Development and sequential analysis of a collagen–chitosan wound management biomaterial. *Romanian Biotechnology Letters* 2019; **24(1)**, 108-117.

[82] W Wei, YH Zhou, HJ Chang and JT Yeh. Antibacterial and miscibility properties of chitosan/collagen blends. *Journal of Macromolecular Science, Part B: Physics* 2015; **54(2)**, 143-158.